Structur analysis of electroless Ni–P–Al_2O_3 nanocomposite coatings

Hong Wang[1, a], Yubao Cao[1,b]

[1] Weifang University, School of Mechanical-electronic and Vehicle Engineering, Weifang 261061, China

[a]sddd69@163.com, [b]wfucyb@163.com

Keywords: Electroless Ni–P; Al_2O_3 nanoparticle; Composite coating; Scanning electron microscopy; X-ray diffraction; Microhardness.

Abstract. Ni–P–Al_2O_3 nano-composite coatings were successfully fabricated on a P20 plastic die steel surface by electroless plating process containing sulfate nickel, sodium hypophosphate and suspended Al_2O_3 nanoparticles. The pH value and temperature of the electroless bath were 4.5 and 87ºC, respectively. The coating was characterized for its microstructure, morphology, microhardness and corrosion resistance. Surface analysis using a field emission scanning electron microscopy (FESEM) showed that the dispersible Al_2O_3 nanoparticles were co-deposited with electroless Ni–P coating onto substrates, the incorporation in Ni–P matrix of Al_2O_3 nanoparticles increases the nodularity of composite coatings. The crystallinity, phases and element distribution of coating were analyzed by X-ray diffraction (XRD) and energy-dispersive X-ray spectroscopy (EDS). It was evident that the X-ray diffraction pattern of the composite coating is similar to that of nanoparticle free coating, both coatings have amorphous structures.

Introduction

Electroless plating is a chemical reduction process, which depends on the catalytic reduction of a metallic ion from an aqueous solution containing a reducing agent, and the subsequent deposition of the metal without the use of electrical energy, this method have many advantages over other coating methods, particularly electrodeposition, such as homogeneous deposition over irregular substrates, simplicity and no need for special equipment. Since the invention of electroless plating technology in 1946 by Brenner and Riddell, electroless nickel has been aroused a surge of research interests by it has proved its supremacy for producing coatings with high corrosion resistance, uniformity of thickness, desired hardness, wear resistance and high cohesion to substrate[1-4]. Due to these desirable characteristics, electroless nickel deposition has been widely used in many industries like electronics board, automotive part, oil and gas instruments and as decorative applications and corrosion resistant coating and so on. To enhance desired properties depending on applications of coating, it has been proposed to deposit composite layer by codepositing various second phase particles using electroless process[5]. Several factors influence the incorporation of hard and soft particles in an electroless Ni-P matrix including particle size and shape, relative density of the particle, particle charge, inertness of the particle, the concentration of particles in the plating bath, the method and degree of agitation, the compatibility of the particle with the matrix, and the orientation of the part being plated.[6, 7]

S.R. Allahkaram et al.[8] reported deposition, characterization and electrochemical evaluation of Ni–P–nanodiamond composite coatings, In their study Ni–P/nano-diamond composite deposition were coated on steel substrate and the optimum concentration of diamond nano-particles was found by study of hardness measurement, linear polarization and electrochemical impedance spectroscopy (EIS). The results demonstrated higher corrosion resistance and greater hardness as compared to the deposited Ni–P. A.S. Hamdy et al.[9] studied the corrosion protection performance of electroless deposited nickel phosphorus (Ni–P) alloy coatings containing tungsten (Ni–P–W) or nano-scattered alumina (Ni–P–Al_2O_3) composite coatings on low carbon steel and the effect of heat treatment on the coating performance. S. Alirezaei et al.[10] investigated the hardness and wear resistance of two types of electroless coating including Ni–P and Ni–P–Al_2O_3 coatings on AISI 1045 steel discs. The results showed that the existence of alumina particles in Ni–P coating matrix led to an increase in the hardness and wear resistance of the deposits. It was also found that heat treated coatings at about 400^o C have the maximum hardness and wear resistance. C. Dehghanian et al.[11] discussed that the effects of the addition of three types of surfactants (cationic, anionic, non-ionic) at different concentrations in the plating bath on the deposition rate, PTFE content and surface morphology of electroless Ni-P/PTFE composite coatings. It was demonstrated that the cationic and non-ionic surfactants created a uniform distribution of PTFE particles in the coatings. The effects of the surfactant type and concentration on the corrosion properties of Ni–P/PTFE coatings were also studied. The corrosion resistance was increased by the incorporation of PTFE particles into the Ni–P matrix. The level of improvement depended largely on the type and concentration of the applied surfactants.

In this work, we reported on the fabrication and characterization of Ni–P–Al_2O_3 electroless composite coatings with applying an outstanding surfactants to obtain optimum concentration of Al_2O_3 nanometer particles in electroless solution and more uniform distributions.

Experimental

Preparation of Ni–P–(nano-Al_2O_3) composite coatings. Commercial plastic die steel P20 specimens (China BAOWU Steel Group Co., Ltd.) with dimension of Φ14 × 2mm, and Al_2O_3 powder (Xuan Cheng Jing Rui New Material Co., Ltd.) with an average size of 100 nm, were used as substrate and reinforcement particles, respectively. To prepare the substrates and make them ready for pretreatment and coating process, they were mechanically polished with emery papers of up to No. 1500 and washed with acetone, ethanol and deionized water several times in an ultrasonic cleaner. Subsequently activated in a 5% (v/v) H_2SO_4 solution for 30 s, followed by rinsed by immersion in distilled water at room temperature for 2 min. Following the pretreatment operation, the specimens were immersed in electroless bath, with chemical composition stated in Table 1, for 3 h. In order to produce a composite coating, the Al_2O_3 concentrated solution with a certain concentration of Al_2O_3 nanoparticles were added to the bath and uniformly dispersed in the solution using a magnetic stirrer.

Table 1 Chemical composition of the electroless deposition bath used.

Bath constituents and parameters	Quantity	Bath constituents and parameters	Quantity
$NiSO_4 \cdot 6H_2O$ (≥98.5%)	25 [g/L]	KI (≥98.5%)	2 [mg/L]
$NaH_2PO_2 \cdot H_2O$ (≥98%)	30 [g/L]	Al_2O_3 concentrated solution	20-100 [mL/L]
$NaCH_3COO$ (≥99%)	20 [g/L]	Temperature	87 ± 2 [°C]
$CH_3CH(OH)COOH$ (85–90%)	20 [mL/L]	pH	4.5 ± 0.2
$C_6H_8O_7 \cdot H_2O$ (≥95%)	8 [g/L]	Time	180 [min]

Structur alanalysis. Phase identification was carried out by an x-ray diffractometer (X' Pert PRO, Netherlands) in θ-2θ geometry using Cu-Ka (λ = 0.15406 nm) radiation over a 2θ angle of 10-100° at a step of 0.02° . The morphologyies and elemental compositions of the coatings were examined by afield emission scanning electron microscope (FESEM; JEOL JSM-6700F, Japan) equipped with an energy-dispersive x-ray spectrometer (EDX).

Evaluation of Coating hardness. Coating hardness measurement, which is reported as an average of five readings on each specimen, was carried out using a micro hardness tester (THVS-10, Beijing TIME High Technology Ltd.) equipped with Vickers indenter under a load of 300g and load exertion time of 15 s.

Results and discussion

Coating morphology. Fig. 1(a) together with Fig. 1(b) show the Al_2O_3 powder used as reinforcement particles are with an average size of 100 nm. Fig. 1(c) shows SEM surface micrographs of mechanically polished P20 Specimen. Fig. 1(d) shows the pattern of EDX of the mechanically polished P20 plastic die steel Specimen, which indicated that the P20 substrate consisted of Cr, Mn and Fe element. Fig. 1(e) shows SEM micrographs of electroless deposited Ni–P composite coating on P20 specimens. This figure reveals that the composite coating possesses a cauliflower type structure as Ni–P coatings do, as well as good homogeneity and high density. Fig. 1(f) indicates that the Ni–P coatings consisted of Ni and P element. The SEM micrograph of the Ni–P–Al_2O_3 composite coating, shown in Fig. 1(g), indicates the presence and favorable distribution of Al_2O_3 particles within entire coating layer, and that the incorporation in Ni–P matrix of nano-Al_2O_3 particles increases the nodularity of composite coatings. The resulting composite coating was measured to contain about 10.7 ± 0.5 Wt% of Al_2O_3 particles. EDX analysis outcomes, presented in Fig. 1(h), strongly suggest the presence of Aluminum and Oxygen elements in the coating.

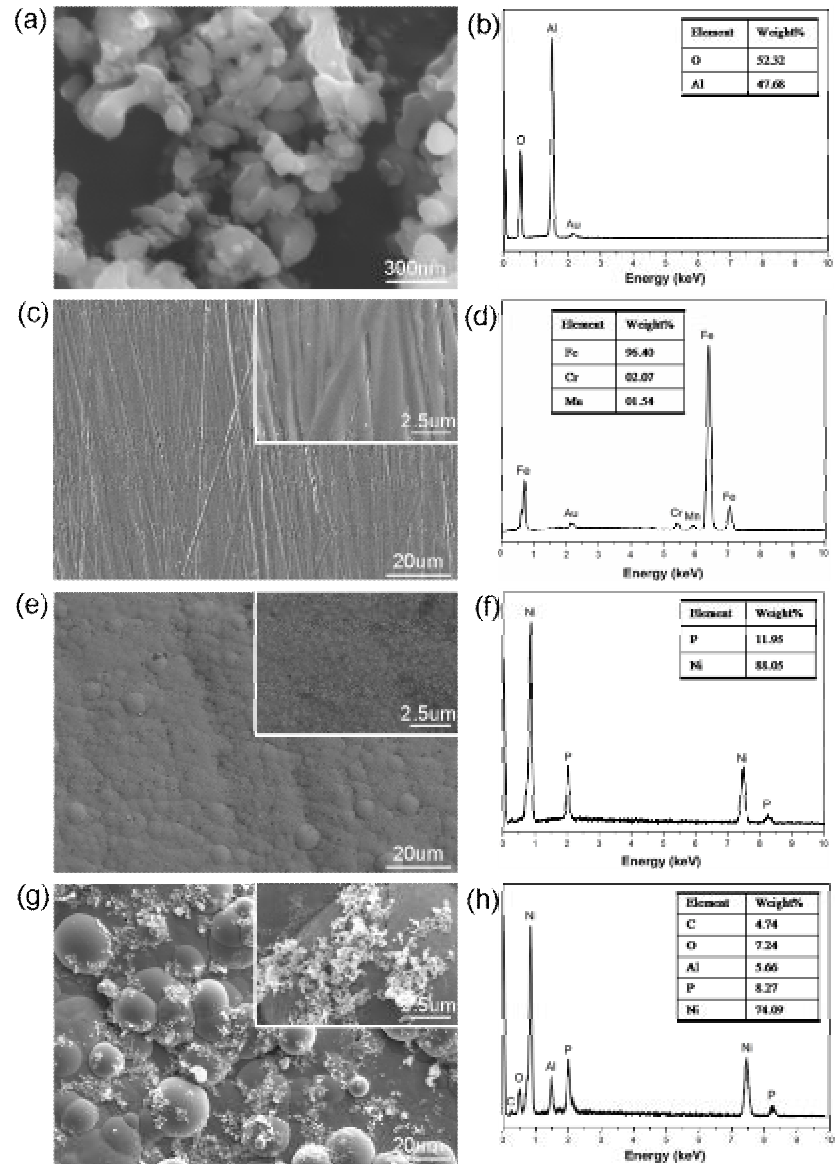

Fig. 1. SEM morphologies (a) together with EDX patterns (b) of Al_2O_3 powder, SEM surface morphologies (c) together with EDX patterns (d) of mechanically polished P20 substrate, SEM surface morphologies (e) together with EDX patterns (f) of electroless Ni–P coating and SEM surface morphologies (g) together with EDX patterns (h) of the Ni–P–Al_2O_3 composite coating.

Coating structure. The X-ray diffraction patterns of as-plated Ni–P, Ni–P–Al_2O_3 deposits and P20 plastic die steel substrate was shown in Fig 3. 3(a) shows the pattern of XRD of the mechanically polished P20 plastic die steel Specimen, which indicated that the substrate consisted of well crystalline body-centered cubic α-Fe phase and the peaks at about 44.5º, 64.9º, 82.1º and 98.7º. The α-Fe crystal diffraction peak intensity ratio $I_{(110)}/I_{(200)}/I_{(211)}/I_{(220)}$ was 100/20/30/10 and corresponded with the data of standard PDF card 6-696. After the electroless Ni–P and Ni–P–Al_2O_3 plating, it can be seen that the α-Fe phase on the substrate surface disappeared because the surface of the substrate was covered with the nickel deposition, see Fig. 2(b-g). The diffraction pattern characteristics of the as-deposited Ni–P and Ni–P–Al_2O_3 composite coatings are similar and they showed broad and high intensity diffraction at about 45º indicating that the coatings are composed of amorphous structure. The well-known amorphous structure of the electroless Ni–P coating is attributed to the distortion of crystal lattice of nickel by the phosphorus atoms[12, 13]. Hence, the incorporation of Al_2O_3 nanoparticles into the Ni–P composite matrix does not affect its crystallinity.

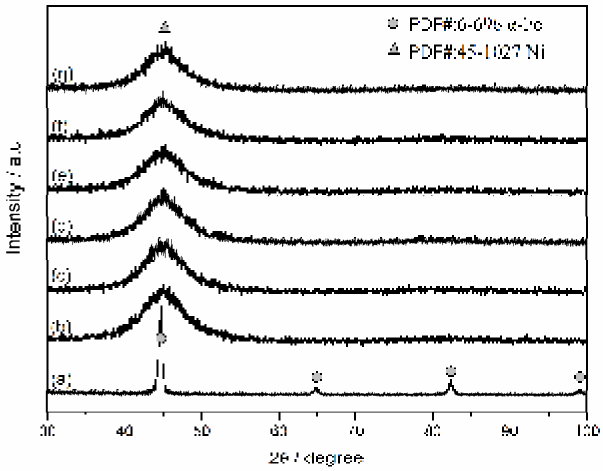

Fig. 2. XRD patterns of P20 plastic die steel(a), electroless Ni–P coating(b), and Ni–P–Al_2O_3 composite coating at various concentrations of nano-Al_2O_3 in electroless solution: 20 mL/L(c), 40 mL/L(d), 60 mL/L(e), 80 mL/L(f), and100 mL/L(g).

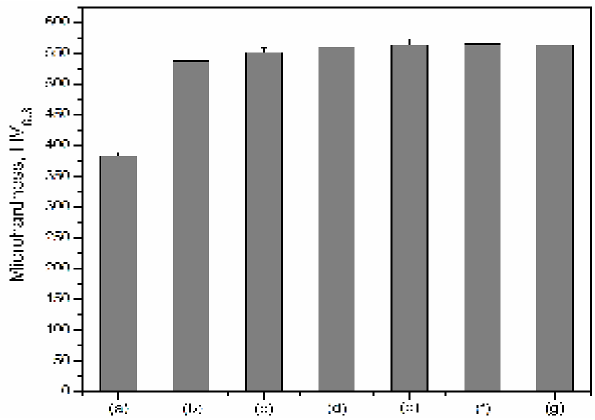

Fig. 3. Microhardness of P20 plastic die steel(a), electroless Ni–P coating(b), and Ni–P–Al_2O_3 composite coating at various concentrations of nano-Al_2O_3 in electroless solution: 20 mL/L(c), 40 mL/L(d), 60 mL/L(e), 80 mL/L(f), and100 mL/L(g).

Coating hardness. The microhardness values measured for the composite coatings were 566.3, 564.7, 563.6, 561.5 and 550.9 $HV_{0.03}$, which were higher than the magnitudes obtained for the Ni–P coating (537.1 $HV_{0.03}$) and substrate alloy P20 (382.5 $HV_{0.03}$). The observed phenomenon can be attributed to the effect of the dispersion strengthening of ceramic particles in the Ni–P matrix. The presence of Al_2O_3 particles inside the composite coating most likely inhibits the movement of dislocations, thus increasing its hardness [14–18].

Conclusions

It was shown that the Ni–P–Al_2O_3 composite coating posses a cauliflower type structure as Ni–P coating, as well as good homogeneity and high density and also has an amorphous structure same as Ni–P coating. The microhardness obtained for the Ni–P–Al_2O_3 composite coatings was 566.3 $HV_{0.03}$, which is much higher than that of what obtained for the substrate alloy P20 (about 382.5 $HV_{0.03}$). All results from the present study have proved that this new method is an effective way to produce nano-composite coatings with high hardness for promising industrial applications.

Acknowledgements

We gratefully acknowledge the financial support provided by the Natural Science Foundation of Shandong Province (Grant No. ZR2011EL003); the Science and Technology Development Program of Shandong Province (Grant Nos. 2011GGX10226 and 2011GGA07173); the Shandong Province Higher Educational Science and Technology Program (Grant No. J11LD56); and the Yuandu Scholar Program of Weifang (Advanced Film and Functional Coating Technology Research Positions).

References

[1] Y.J. Hu, L. Xiong and J.L. Meng: Appl. Surf. Sci. Vol. 253 (2007), p. 5029–5034.
[2] D. Dong, X.H. Chen, W.T. Xiao, G.B. Yang and P.Y. Zhang: Appl. Surf. Sci. Vol. 255 (2009), p. 7051–7055.
[3] T. Rabizadeh, S.R. Allahkaram and A. Zarebidaki: Mater. Des. Vol. 31 (2010), p. 3174–3179.
[4] K.H. Krishnan, S. John, K.N. Srinivasan, J. Praveen, M. Ganesan and P.M. Kavimani: Metall. Mater. Trans. A Vol. 37 (2006), p. 1917–1926.
[5] I. Apachitei, J. Duszczyk, L. Katgerman and P.J.B. Overkamp: Scripta Mater. Vol. 38 (1998), p. 1383–1389.
[6] J.N. Balaraju, T.S.N. Sankara Narayanan and S.K. Seshadri: J. Appl. Electrochem. Vol. 33 (2003), p. 807–816.
[7] J.N. Balaraju, B. Kalavati and K.S. Rajam: Surf. Coat. Technol. Vol. 200 (2006), p. 3933–3941.
[8] H. Mazaheri and S.R. Allahkaram: Appl. Surf. Sci. Vol. 258 (2012), p. 4574–4580.
[9] A.S. Hamdy, M.A. Shoeib, H. Hady and O.A. Salam: Surf. Coat. Technol. Vol. 202 (2007), p. 162–171.
[10] S. Alirezaei, S.M. Monirvaghefi, M. Salehi and A. Saatchi: Wear Vol. 262 (2007), p. 978–985.
[11] I.R. Mafi and C. Dehghanian: Appl. Surf. Sci. Vol. 257 (2011), p. 8653–8658.
[12] R.C. Agarwala, V. Agarwala and R. Sharma: Synth. React. Inorg. Met.-Org. Chem. Vol. 36 (2006), p. 493–515.
[13] S.B. Sharma, R.C. Agarwala, V. Agarwala and K.G. Satyanarayana: J. Mater. Sci. Vol. 37 (2002), p. 5247–5254.
[14] M. Ebrahimian-Hosseinabadi, K. Azari-Dorcheh and S.M. Moonir Vaghefi: Wear Vol. 260 (2006), p. 123–127.
[15] Y. Yang, W. Chen, C. Zhou, H. Xu and W. Gao: Appl. Nanosci. Vol. 1 (2011), p. 19–26.
[16] Y.W. Song, D.Y. Shan, R.S. Chen and E.H. Han: Surf. Eng. Vol. 23 (2007), p. 334–338.
[17] F. Hou, W. Wang and H. Guo: Appl. Surf. Sci. Vol. 252 (2006), p. 3812–3817.
[18] Z. Zhang, D.L. Chen: Scr. Mater. Vol. 54 (2006), p. 1321–1326.